REINFORCED CONCRETE BRIDGE DECK REPAIR WITH TITANIUM NSM

S.L. Platt[1*], K.A. Harries[2] and M.J. McCabe[3]

[1] *Architecture & Civil Engineering, University of Bath, Bath, BA2 7AY, UK*
[2] *Civil & Environmental Engineering, University of Pittsburgh, Pittsburgh, 15260, USA*
[3] *United States Department of Agriculture Forest Service, Montana, USA*

**Correspondence E-mail: S.L.Platt@bath.ac.uk, TP: +44 (0)7568648939*

Abstract: The use of titanium bars as a near surface mounted (NSM) repair method for highway bridge deck slabs is investigated in this pilot study. Four full-scale slabs had half of their internal reinforcing steel cut resulting in an approximately a 40% loss of slab capacity; these represented 'damaged' slabs. The objective of this study was to evaluate the performance of replacing these two cut bars in order to restore the original capacity of the slab. The four slabs were repaired using NSM titanium bars designed to restore either their capacity or stiffness of the cut bars. One slab from each group was repaired using a full-length straight bar while the other implemented a 'staple' type repair. Both approaches effectively restored the capacity of the slabs although each had significant impacts on the available ductility of the repaired slab. Repairs based on restoring lost bar strength resulted in preferable behavior. Restoring lost stiffness required four times as much titanium and resulted in over-reinforced sections showing little ductility.

Keywords: Concrete; Corrosion; Retrofit; Bond; Ti6Al-4V; Serviceability

1. Introduction

Titanium reinforcing bars for concrete rehabilitation have been proposed (Adkins and George 2017) and demonstrated in laboratory tests (Platt and Harries 2018a and 2018b). The primary advantage and motivation for using titanium is its corrosion resistance. An anticipated application for titanium reinforcement is near surface mounted (NSM) reinforcement for strengthening reinforced concrete members in cases where the advantages of titanium may be realized such as in highly corrosive environments, non-magnetic applications, and others in which ductility or high service temperatures may be required.

A single demonstration application is known (Higgins et al. 2015 and 2017) in which NSM titanium 'staples' – straight bars having a 90 degree bend at either end to affect anchorage – were used in a bridge application.

The fundamental material behaviours of titanium are similar in form to those of steel. Titanium, like steel, exhibits an elastic behaviour to a proportional limit, a definable yield value followed, typically, by some degree of strain hardening, and displays a great deal of ductility in most cases. This pilot study is part of a large study investigating specific aspects of the use of 6Al-4V titanium (UNS designation R56400) bars having ribbed deformations as a concrete reinforcing material (Platt 2018). When compared to conventional ASTM A615 reinforcing steel, Ti6Al-4V exhibits nearly double the yield strength and half the extensional modulus. Titanium reinforcing bars used in this study were nominally #5 bars, having a nominal diameter and area of 15.9 mm and 200 mm^2, respectively. Results of tension tests compliant with ASTM A370-14 (including Annex A9) in all ways, other than being titanium, are shown in Figure 1. Nominal (for design) and measured material properties of the bars used in this study are shown in Table 1.

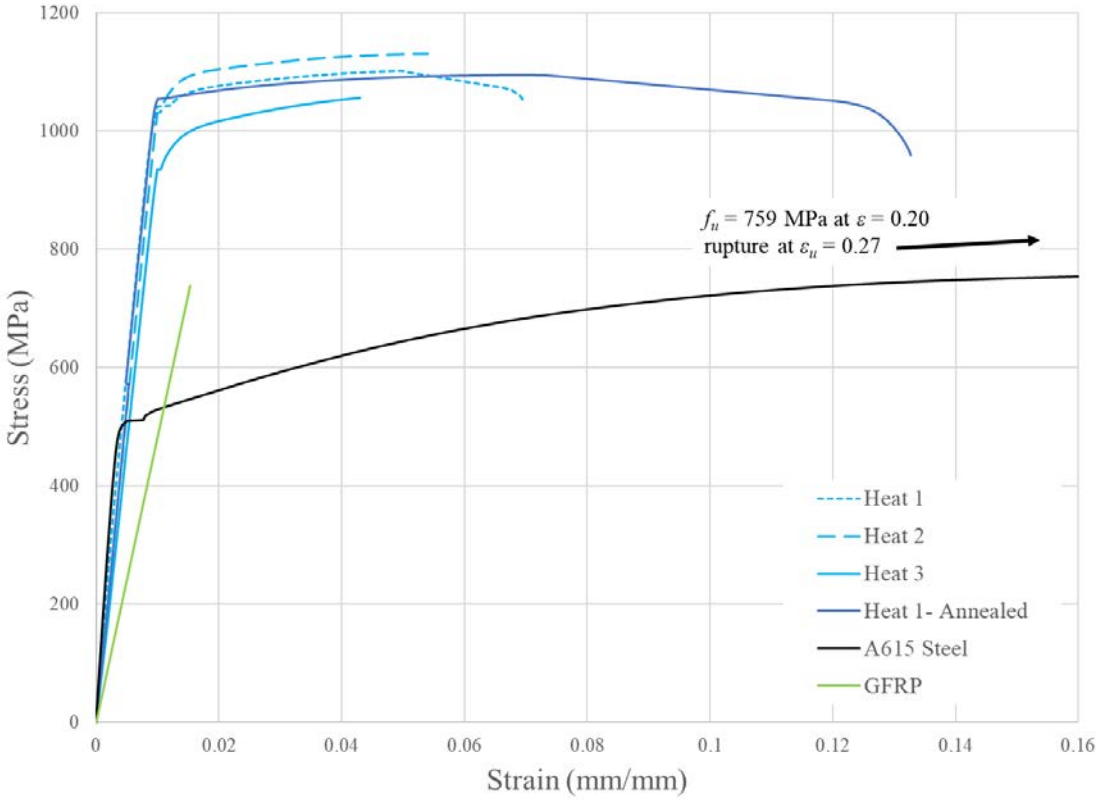

Figure 1 Representative experimentally determined stress-strain curves.

Table 1 Geometric and mechanical properties of reinforcing bars reported in this study

	#5 6Al 4V Titanium bars		# 5 ASTM A615 Steel bars	
	nominal properties	measured properties (Platt and Harries 2018a)	nominal properties	measured properties (McCabe et al. 2014)
bar area	200 mm²	236 mm²	200 mm²	
bar diameter	15.9 mm	17.4 mm	15.9 mm	
density	4430 kg/m³	4407 kg/m³	7900 kg/m³	
modulus	E_{Ti} = 114 GPa		E_s = 200 GPa	
yield strength	f_{yTi} = 965 MPa	f_{yTi} = 999 MPa	f_{ys} = 414 MPa	f_{yTi} = 467 MPa
tensile strength	f_{uTi} = 1100 MPa	f_{uTi} = 1054 MPa	f_{us} > 586 MPa	f_{uTi} = 744 MPa
elongation at rupture	ε_{Tiu} > 0.100	ε_{Tiu} > 0.084	ε_{su} > 0.150	

6Al-4V titanium bars exhibit yield strength approximately twice that of ASTM A615 reinforcing steel and an extensional modulus about 55% of steel. As such, the yield strain of Ti6Al-4V is on the order of 0.008, approximately four times greater than A615 steel. The softer response affects the assumed concrete behaviour and can be a significant disadvantage when considering serviceability; primarily in the form of increased crack widths.

The behaviour of reinforcing steel, particularly under service loads, is a function of axial stiffness, *EA*; thus to directly replace steel with titanium, twice as much titanium is required. Typically, this will not be practical. Alternatively, the design paradigm used for glass fibre-reinforced polymer (GFRP) reinforcing bars (ACI 440.1R) , which presents an elastic behaviour to failure with modulus ranging from 20% to 50% that of steel, may be used for titanium-reinforced concrete or for using titanium as a retrofit reinforcement.

2. NSM Titanium slab tests

Four steel-reinforced bridge deck slabs, cast in 2013, were available to develop a pilot study to demonstrate the efficacy of titanium NSM retrofit. These slabs were designed based on the AASHTO (2017) prescriptive design method and had four #5 primary reinforcing bars spaced at 140 mm, top and bottom, across the 559 mm slab width. The 'control' specimen used for this study is Slab A, tested in 2013 (McCabe 2013; McCabe et al. 2014). Details of the slab geometry are shown in Figure 2.

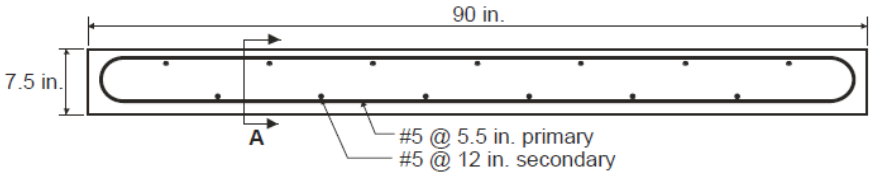

a) elevation of slab detail

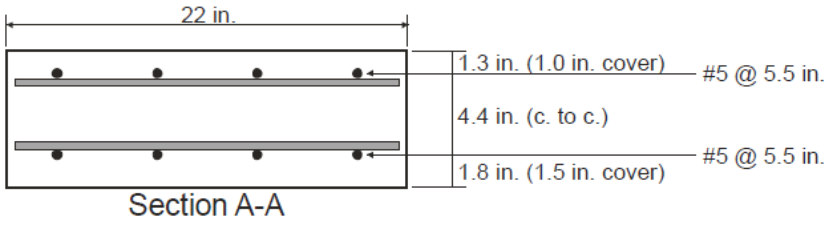

b) end elevation (Section A-A) of slab detail

Figure 2 Details of laboratory control specimen (McCabe 2013) (1 in. = 25 mm)

Each of the four slabs to be retrofit was 'damaged' by cutting two of the four existing #5 steel bars at increments along their length sufficient to ensure that the bars no longer contributed to the flexural capacity of the slabs. The slabs were then repaired with one of two types of NSM repairs: a straight NSM bar or an NSM 'staple'. The staples, as shown in Figure 3, were short lengths of NSM bar having 90 degree anchorages at either end. Such a staple may be practical for repairing local damage (as was the case in this study) or in locations were straight bar development is not possible.

Two scenarios are investigated based on repairs that restore either the capacity ($A_s f_{ys} = A_{Ti} f_{yTi}$) or equivalent stiffness ($A_s E_s = A_{Ti} E_{Ti}$) of the cut bars. In either case, #5 titanium deformed bars were embedded within channels cut along the length of the tension face of the slabs. Sikadur 31 (a commercially available two-part structural adhesive) was used to embed the bars. The installations, shown in Figure 3, were, other than the use of titanium, compliant with the design approach of ACI 440.2R-17.

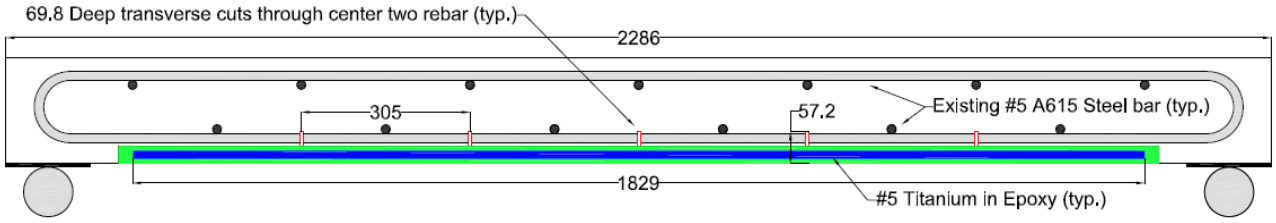

TiNSM-1 and TiNSM-2 elevation with NSM titanium straight bars (units = mm)

NSM channels on [inverted] slab soffit; transverse cuts through internal reinforcing bars can also be seen.

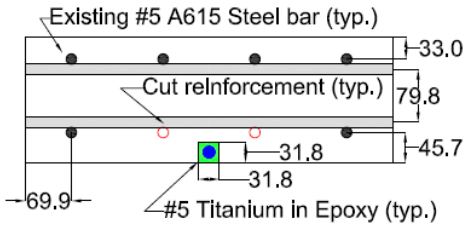

TiNSM-1 section – 1 bar centered in slab soffit

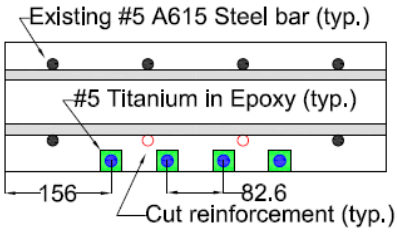

TiNSM-2 section – 4 bars at 83 mm across soffit

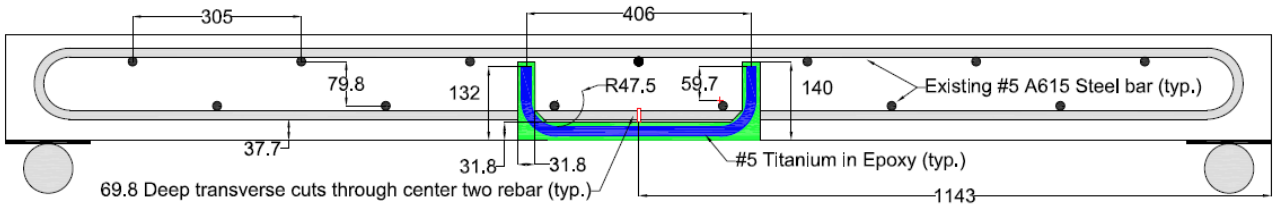

TiNSM-3 and TiNSM-4 elevation with NSM titanium staples (units = mm)

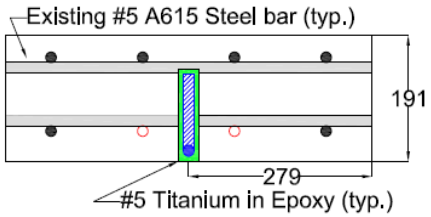

TiNSM-3 section – 1 staple centered in slab soffit

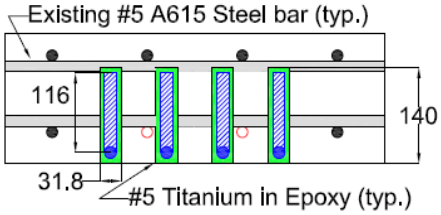

TiNSM-4 section – 4 staples at 83 mm across soffit

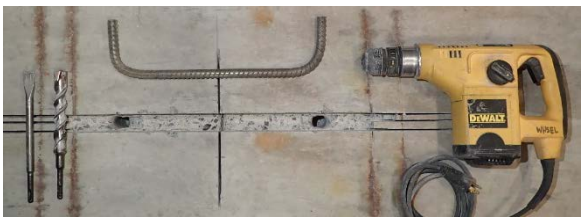

Staple, channel and installation tools

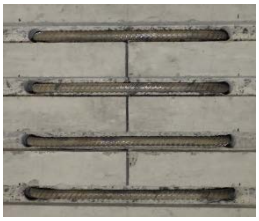

TiNSM4 staples before epoxy embedment

Figure 3 Repaired cross sections and elevations of slabs based on Strength (TiNSM 1 and 3) and Service (TiNSM 2 and 4) criteria (all dimensions in mm).

After allowing the NSM installations to cure for a minimum of 72 hours, they were placed in a test frame. Loading and support conditions, shown in Figure 4a, were identical to those used to test control Slab A (McCabe 2013). The slabs were tested in mid-point flexure over a simple span length (L) of 2135 mm. Primary instrumentation consisted

of multiple DEMEC gauges, having a resolution of 8 microstrain and gauge length of 8 in. (203.2 mm), arranged vertically at midspan (Figure 4).

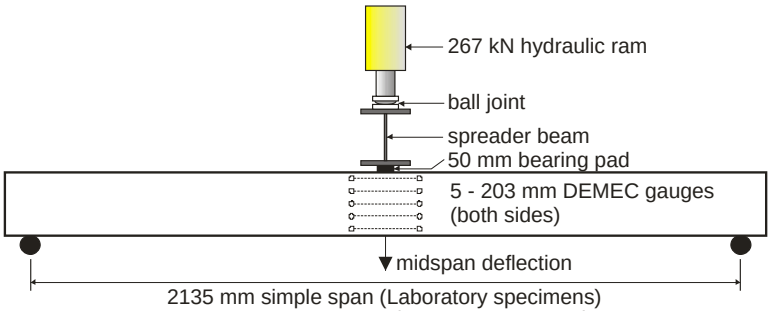

test Set-up (Slab A shown)

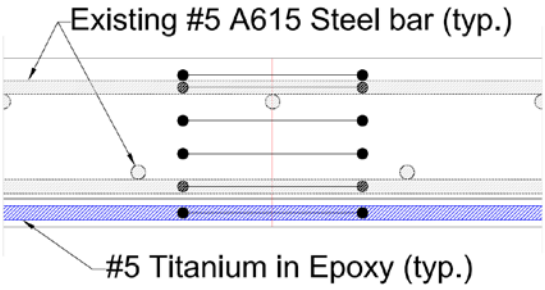

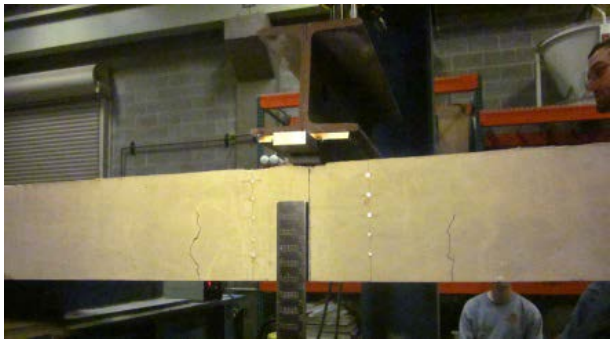

DEMEC and vertical deflection instrumentation (Slab A shown)

Figure 4 Test Set-Up and Instrumentation

Tests of the four NSM titanium retrofit slabs were carried out in a manner (to the extent possible) identical to the control specimen: Slab A reported previously by McCabe et al. (2014).

Load was applied using a 267 kN capacity hydraulic cylinder; load was measured with a precision of 320 N. Load was applied at intervals of approximately 4.45 kN while midspan displacement was recorded manually at each load interval with a precision of 0.8 mm.

Since there were no test cylinders remaining from the original casting of the slabs and due to undocumented environmental conditions during storage, core samples were taken from the slabs to confirm present *in situ* compressive and tensile strengths. Cores having a diameter of 57 mm (2.25 in.) were removed from the [essentially undamaged] support region of the slabs following testing. The compression and tension strengths obtained from the 57 mm cores (including all corrections) are shown in Table 2. An expected increase in compressive strength is observed. The 1666 day tested strengths reported in Table 2 were used for all subsequent analyses of the slabs. The 132-day strength was used for Slab A. Internal reinforcing steel and NSM titanium material properties are reported in Table 1.

Table 2 Summary of concrete properties

Age	ASTM C39			ASTM C496			ASTM C78		
	Compression test			Split Cylinder test			Modulus of rupture		
days	n	f_c'	COV	n	f_{sp}	COV	n	f_r	COV
28[a]	3	44.8 MPa	0.034	3	3.12 MPa = $0.47\sqrt{f_c'}$	0.131	3	5.45 MPa = $0.81\sqrt{f_c'}$	0.056
132[a]	3	45.8 MPa	0.084	-	-	-	-	-	-
1666[b]	8	50.7 MPa	0.081	5	2.98 MPa = $0.42\sqrt{f_c'}$	0.186	-	--	-
[a] McCabe (2013) [b] Platt (2018)									

3. Test Results

The key results for NSM-repaired slabs and the control Slab A are presented in Table 3. Plots of applied moment versus curvature at midspan are shown in Figure 5. The reported moments are calculated as: M = PL/4, were P includes the cross-head contribution but neglects the weight of the slab. The curvature is calculated by dividing the difference in strain between the uppermost DEMEC gauge and the gauge located at the existing A615 steel tension reinforcement by the vertical distance separating these gauges. This is consistent with the procedure used for the control Slab A.

Table 3 Summary of tested slabs

Slab		A	TiNSM-1	TiNSM-2	TiNSM-3	TiNSM-4
depth of slab	mm	191	216	191	191	191
design condition			strength: $A_s f_{ys} + A_{Ti} f_{yTi}$ ≈ Slab A	stiffness: $A_s E_s + A_{Ti} E_{Ti}$ ≈ Slab A	strength: $A_s f_{ys} + A_{Ti} f_{yTi}$ ≈ Slab A	stiffness: $A_s E_s + A_{Ti} E_{Ti}$ ≈ Slab A
NSM bars		none	1 - #5 straight bar	4 - #5 straight bars	1 - #5 staple	4 - #5 staples
load at first crack	kN	22.6	23.1	28.2	28.2	32.6
moment at first crack	kN-m	12.1	22.1	15.0	15.0	17.4
load at steel bar yield	kN	81.0	81.8	104	72.5	113
moment at steel bar yield	kN-m	43.1	43.6	55.3	38.7	60.1
ratio yield capacity to Slab A	-	-	1.01 0.89[1]	1.28	0.90	1.39
deflection at steel bar yield	mm	9.65	5.59	6.35	5.59	11.2
curvature at steel bar yield	rad/km	25.6	16.6	21.2	18.4	14.4
ultimate load	kN	125	179	192	117	130
ultimate moment	kN-m	66.6	95.7	103	62.5	69.6
ratio ultimate capacity to Slab A	-	-	1.44 1.12[1]	1.55	0.94	1.05
deflection at ultimate load	mm	-	32.5	15.0	25.4	31.0
failure mode		flexural	flexural	shear	flexural	flexural at end of staples

[1] value normalized to 191 mm slab depth; i.e.: Slab TiNSM-1 ratio multiplied by $(191/216)^2$

The behavior of all slabs was analyzed using the program RESPONSE (Bentz 2000). All material properties used in the RESPONSE models are the measured values given in Tables 1 and 2. Figure 6 shows the predicted moment-curvature responses superimposed with the as tested results.

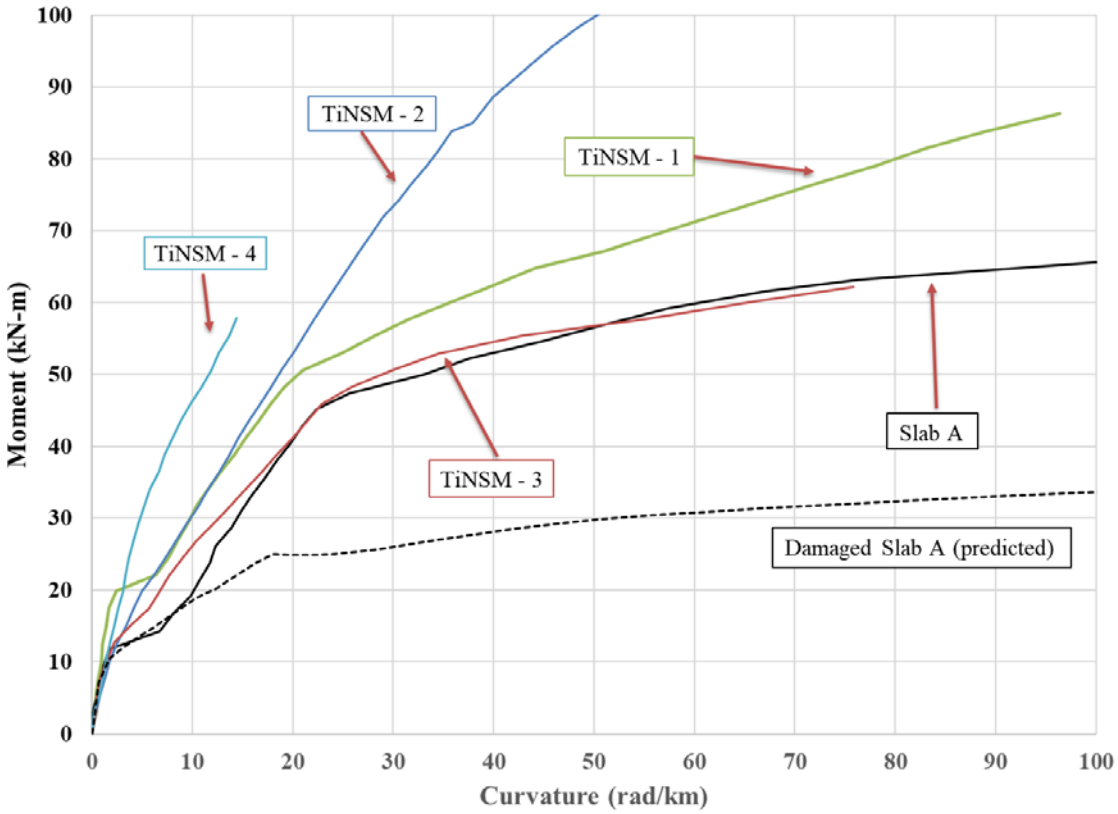

Figure 5 Summary of Moment-Curvature results from slab flexure tests

The predicted moment-curvature responses are for midspan performance; effects of shear-moment interaction along the relatively short shear spans will result in a marginal reduction of the predicted "pure" moment capacity. In the more heavily reinforced Slabs TiNSM2 and 4, the retrofit flexural capacity exceeds the slab shear capacity and the latter controls the ultimate behavior. RESPONSE-predicted capacities are shown in Table 4.

Table 4 Summary of predicted capacities of NSM-reinforced slabs

	Slab A	Slab A with two bars cut	TiNSM-1	TiNSM-3	TiNSM-2	TiNSM-4
Predicted moment capacity (kNm)	57.3	34.3	84.1	65.6	134	
Predicted peak applied load (kN)	94.8	52.4	137	100	154	
moment capacity accounting for shear (kNm)	50.5	27.9	72.8	53.5	82.3	
Observed moment capacity (kNm)	66.6	-	84.6[1]	62.5	103	69.6
Capacity normalized to Slab A	1.0	-	1.27	0.94	1.55	1.05

[1] value normalized to 191 mm slab depth; i.e.: Slab TiNSM-1 ratio multiplied by $(191/216)^2$

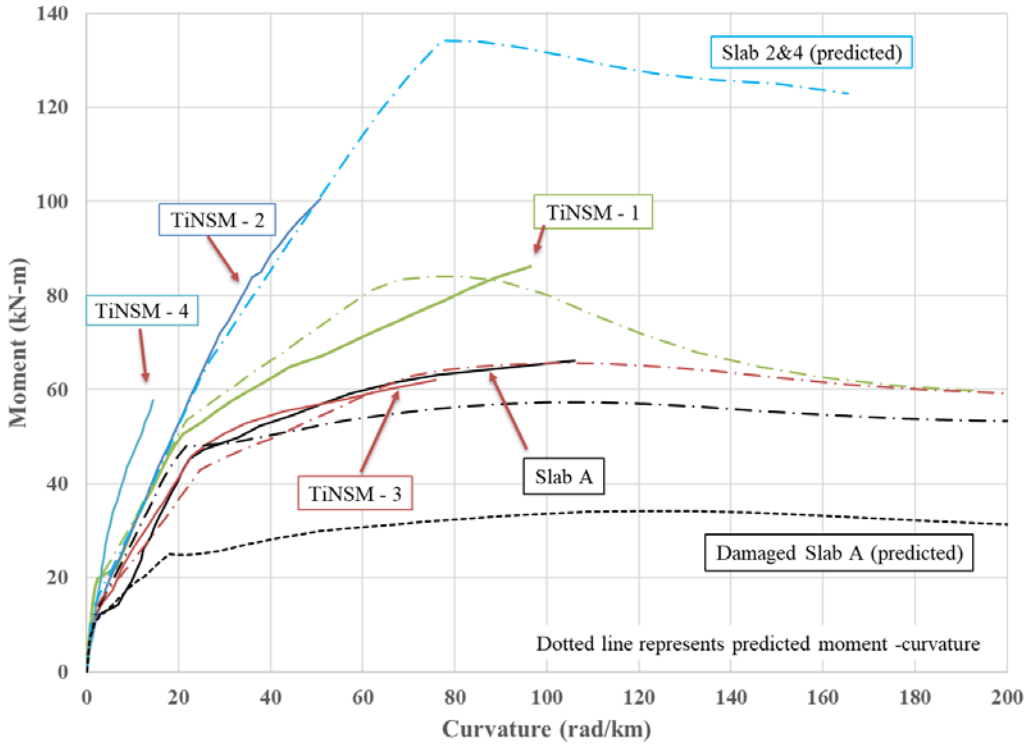

Figure 6 Summary of Moment-Curvature results with RESPONSE predicted results

The proposed staple repair was investigated on two slabs having two of the four #5 ASTM A615 reinforcing bars cut only at midspan (Figure 4). This effectively dropped the capacity of the slab approximately 40% (Table 4). The development length for a #5 bar is l_d = 340 mm. Thus not until 340 mm to either side of midspan, is the capacity of the cut #5 bars theoretically redeveloped. The staples used were only 406 mm long and thus did not span the entire region of reduced capacity (680 mm). Figure 7 describes the resulting moment capacity envelopes (normalized to the predicted capacity of Slab A). The applied moments at failure are shown by the dashed lines. Clearly Slab A is critical at midspan, as is TiNSM-3, although there is a relatively small margin at the end of staple. The applied moment of TiNSM-4 is seen to intersect its capacity envelope at the end of the staples, rather than at the increased midpsan capacity. Thus, the staples in this case were too short to develop the predicted capacity of the repaired slab, as reflected in Table 3.

To mitigate the potential weak section at the staple anchorage, the anchorage should be located beyond the point where the cut bars have been fully redeveloped. That is, the staple length should exceed $2l_d$ (of the cut/damaged bars).

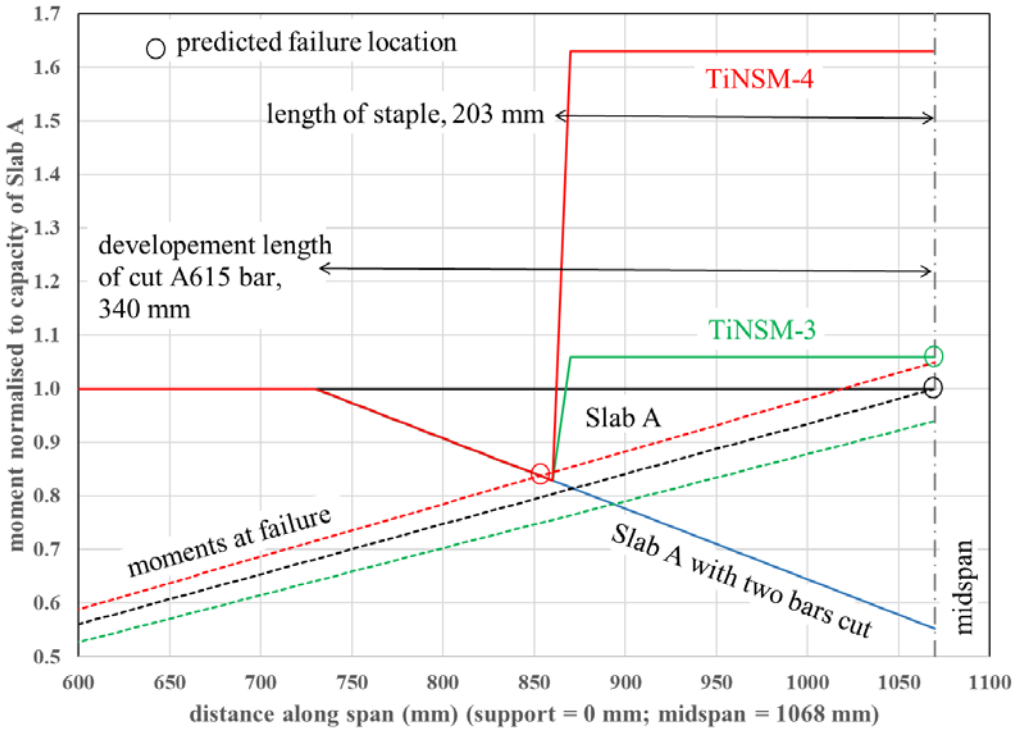

Figure 7 Generalized capacity envelope of the damaged slab with and without staple repair

4. Conclusion

The application of titanium NSM reinforcement was investigated through a pilot study using four intentionally damaged steel-reinforced bridge deck slabs. Both straight bar repairs and the staple repair based on equivalent stiffness (4 staples) restored the original slab capacity. The repair having the single titanium staple, theoretically sufficient to restore the capacity lost by cutting the internal reinforcement, restored only 94% of the original slab capacity. It is hypothesized that if the staples had been designed to extend beyond the development length of the cut internal steel reinforcing bars, the resulting performance of the NSM repairs would have been improved.

The slabs having only a single titanium bar, developed ductility similar to the undamaged control Slab A although exhibited significant slip at ultimate capacity. The slabs having four bars were both effectively over-reinforced leading to increased capacity but decreased ductility. The slab having four full-length titanium NSM bars, failed upon reaching its shear capacity whereas that having four staples failed 'prematurely' in flexure at the section at the end of the staples. The staples were not long enough to develop the full theoretical capacity of this slab.

Cost of titanium bars

Currently the associated costs of implementing titanium as a reinforcement material must be overcome. On a unit weight basis, 6Al-4V titanium bars are approximately 15 times more expensive than A615 steel bars and 5 times more expensive than solid stainless steel bars (Platt 2018; Triantafillou 2012). However, the final in-place cost of titanium bars will be affected by the design paradigm. Platt and Harries (2019) report a preliminary study of the cost of using #5 6Al-4V titanium bars for bridge deck reinforcement (based on an earlier study by Triantafillou (2012) that considered several other bar materials). Depending on the design paradigm used, 6Al-4V reinforcing bars were estimated to cost between \$430/m² [of bridge deck constructed] and \$1700/m². A615 bars were estimated to cost \$117/m² and solid stainless steel bars were \$294/m². The typical bridge construction unit cost for medium span bridges using conventional A615 reinforcing bars (in 2010) was \$989/m² (Triantafillou 2012). Therefore, the use of titanium bars

represents a significant cost premium although this may be offset by long term savings in maintenance for a non-corrosive deck.

Acknowledgement

The research presented was sponsored by the Perryman Company. The findings and conclusions reported in this paper reflect the opinion of the authors and are not necessarily those of the Perryman Co. Slab construction and testing Slab A was sponsored by the Pennsylvania Department of Transportation. All testing was conducted in the Watkins Haggart Structural Engineering Laboratory at the University of Pittsburgh. The second author acknowledges the support of the Leverhulme Trust (UK).

References

AASHTO (2014) *LRFD Bridge Design Specifications* (7th edition), American Association of State Highway and Transportation Officials.

ACI 440.2R-17 *Design and Construction of Externally Bonded FRP Systems*, American Concrete Institute.

ACI 440.1R-15 (2015) *Guide for the Design and Construction of Structural Concrete Reinforced with FRP Bars*, American Concrete Institute.

Adkins, J. and George, W. (2017) Titanium Finds a Home in Civil Engineering, *Concrete International*, December 2017, pp 51-55.

ASTM A370-14 (2014) *Test Methods and Definitions for Mechanical Testing of Steel Products*, ASTM International.

ASTM A615-16 (2016) *Standard Specification for Deformed and Plain Carbon-Steel Bars for Concrete Reinforcement*, ASTM International.

ASTM C39-16 (2016) *Standard Test Method for Compressive Strength of Cylindrical Concrete Specimens*, ASTM International.

ASTM C496-11 (2011) *Standard Test Method f or Splitting Tensile Strength of Cylindrical Concrete Specimens*, ASTM International.

Bentz E. (2000) *Sectional Analysis of Reinforced Concrete Members*, PhD Thesis, Department of Civil Engineering, University of Toronto, 2000, 310 pp.

Higgins, C. (2015) Titanium Reinforcing for Strengthening RC Bridges, *International Bridge Conference*, Pittsburgh, PA, June 2015.

Higgins, C. Knudtsen, J. Amneus, D. and Barker, L. (2017) Shear and Flexural Strengthening of Reinforced Concrete Beams with Titanium Alloy Bar, *Proceedings of the 2nd World Congress on Civil, Structural, and Environmental Engineering (CSEE'17)*, Barcelona, Spain, Apr. 2017.

Higgins, C. Amneus, D. and Barker, L. (2015) Methods for Strengthening Reinforced Concrete Bridge Girders Containing Poorly Detailed Flexural Steel Using Near-Surface Mounted Metallics, Report No. *FHWA-OR-RD-16-02*, Oregon Department of Transportation, Salem, OR, 138 pp.

McCabe, M., Harries, K.A. and Sweriduk, M. (2014). Evaluation of Concrete Bridge Deck Rehabilitation by the Method of Hydrodemolition and Latex-Modified Overlay. *Proceedings of 15th International Conference on Structural Faults and Repair,* London.

McCabe, M. (2013). *Structural Evaluation of Slab Rehabilitation by Method of Hydrodemolition and Latex Modified Overlay*. (Master's thesis), University of Pittsburgh, PA.

Platt, S. and Harries, K.A. (2019; in revision) Proposed Flexural Design Methodology for Titanium Reinforcing Bars in Concrete, *Engineering Structures*

Platt, S. (2018a) *Development of Titanium Reinforcing Bars for Concrete and Masonry*, Doctoral dissertation, University of Pittsburgh.

Platt, S. and Harries, K.A. (2018b) Geometry, Material Properties and Bond Performance of Titanium Reinforcing Bars, *Construction and Building Materials*, **187**, 1253-1266.

Platt, S. and Harries, K.A. (2018) Study of Galvanic Corrosion Potential of NSM Titanium Reinforcing Bars, *Case Studies in Construction Materials* **9**, e00175.

Triantafillou. L (2012) Cost Comparison of Corrosion Resistant Reinforcing Steel – Deployment Considerations, *FHWA Office of Infrastructure Research and Development* as updated by Wong, W. (2014)